Radiation Measurements 43 (2008) 1525–1531

Contents lists available at ScienceDirect

Radiation Measurements

journal homepage: www.elsevier.com/locate/radmeas

Performance of GEANT4 in dosimetry applications: Calculation of X-ray spectra and kerma-to-dose equivalent conversion coefficients

Carla C. Guimarães [a], Maurício Moralles [b], Emico Okuno [a,*]

[a] Laboratório de Dosimetria, Instituto de Física da Universidade de São Paulo, DFN, CP 66318, CEP 05315-970 São Paulo, SP, Brazil
[b] Centro do Reator de Pesquisas, Instituto de Pesquisas Energéticas e Nucleares, CP 11049, CEP 05422-970 São Paulo, SP, Brazil

ARTICLE INFO

Article history:
Received 2 October 2007
Received in revised form 15 April 2008
Accepted 9 July 2008

PACS:
87.58.Sp
87.64.Aa
87.66.−a

Keywords:
Monte Carlo
GEANT4
Dose equivalent
Conversion coefficient

ABSTRACT

In order to validate the Geant4 toolkit for dosimetry applications, simulations were performed to calculate conversion coefficients $h(10, \alpha)$ from air kerma free-in-air to personal dose equivalent $H_p(10, \alpha)$. The simulations consisted of two parts: the production of X-rays with radiation qualities of narrow and wide spectra, and the interaction of radiation with ICRU tissue-equivalent and ISO water slab phantoms. The half-value layers of the X-ray spectra obtained by simulation were compared with experimental results. Mean energy, spectral resolution, half-value layers and conversion coefficients were compared with ISO reference values. The good agreement between results from simulation and reference data shows that the Geant4 is suitable for dosimetry applications which involve photons with energies in the range of ten to a few hundreds of keV.

1. Introduction

Stimulated by the continuous advances in computer technology, the employment of Monte Carlo methods in simulations of complex problems has been increased in the last decades. Continuous efforts of several groups in the world culminated with a variety of Monte Carlo codes that treat the radiation transport in matter allowing precise calculations in the fields of medical physics, dosimetry and radiation protection.

The personal dose equivalent $H_p(d, \alpha)$ is a protection quantity that can be evaluated using Monte Carlo calculations. According to the ICRU Report 57 (ICRU, 1998), for monitoring purposes, the operational quantity $H_p(d, \alpha)$ provides reasonable evaluation of the dose equivalent in the soft tissue at a depth d, where α is the angle between the normal reference direction of the dosimeter and the direction of radiation incidence. Since the protection quantities are not directly measurable and the instruments for radiation monitoring need to be calibrated in terms of a measurable quantity, conversion coefficients $h(d, \alpha)$ are calculated to relate some basic physical quantities, like fluence or air kerma free-in-air (K_{air}), to the operational quantities. In addition, $H_p(d, \alpha)$, originally defined as a quantity in the human body, is extended to phantoms for practical reasons in calibration procedures. These reference conversion coefficients were calculated by several methods and they are described in ICRU Report 57 (ICRU, 1998), and ISO reports 4037-3 (ISO, 1999) and 4037-4 (ISO, 2004), for phantoms irradiated under ideal conditions using unidirectional beams of standard radiation qualities.

Although the reference conversion coefficients are useful in calibration procedures, difficulties arise when the conditions of irradiation differ from the ones recommended in technical reports. In realistic situations, workers are exposed to radiation with broad spectrum, and their personal dosimeters receive photons from all directions. Thus, the availability of a confident tool for the calculation of conversion coefficients for customised conditions of irradiation would be very appropriate and useful. The potential application of this tool can be found in recently published studies. To mention two examples, predictions of the response of commercially available $H_p(10)$ chambers (Mikami et al., 2007) and conversion coefficients for new proposed radiation qualities (Ankerhold, 2007) could be performed with Monte Carlo calculations.

In this study, the Geant4 Monte Carlo toolkit (Agostinelli et al., 2003) was employed to calculate conversion coefficients for several irradiation conditions. Differently from other calculations, which used either monoenergetic radiation (Grosswendt, 1991a,b) or

* Corresponding author. Tel.: +55 11 30916994; fax: +55 11 30912742.
E-mail address: emico.okuno@dfn.if.usp.br (E. Okuno).

1350-4487/$ – see front matter © 2008 Elsevier Ltd. All rights reserved.
doi:10.1016/j.radmeas.2008.07.001

photons with energy distributions determined experimentally (Grosswendt, 1992; Ankerhold et al., 1999), in the present work the X-ray spectra were also obtained using the Monte Carlo method. In this way, the performance of Geant4 to treat the physical processes that are predominant in dosimetry of X-rays was verified.

The simulation was performed in two stages. In the first one, the primary particles consist of electrons that interact with the anode of the X-ray tube by ionisation, bremsstrahlung and multiple scattering processes. The transport of bremsstrahlung and characteristic radiation through the anode and absorbers is also performed to produce the X-ray spectra of standard radiation qualities. In the second part, the interaction of photons with phantoms was simulated for different incidence angles, and conversion coefficients were calculated for the depth of 10 mm.

2. X-ray spectra

In this section, characteristics of X-ray spectra of the ISO narrow and wide series radiation qualities obtained by simulation are compared with experimental results and also with reference values of the ISO reports (ISO, 1997, 2004), hereinafter referred as reference data.

2.1. Experiment

The X-ray beams were produced with a Philips MG 450 system, which has a tungsten anode with angle of 22° and inherent filtration of 2.2 mm beryllium. Aluminium, copper, tin and lead absorbers were employed to produce beams with the ISO radiation qualities (ISO, 1997). The HVLs were obtained using aluminium and copper absorbers, and two cylindrical ionisation chambers: the 0.6 cc Farmer type NE 2571 (Nuclear Enterprise) and the 10 × 5–6 Radcal ion chamber (Radcal Corporation) placed at the distance of 1.20 m from the focal point. The purity of the absorbers is 99.98% for Al and approximately 99.5% for Cu absorbers and additional filtration.

The dependence of the measured air kerma on the thickness x of the absorber was adjusted with two exponentials, according to the equation

$$K_{\mathrm{air}} = A_1 \exp\left(-\frac{x}{t_1}\right) + A_2 \exp\left(-\frac{x}{t_2}\right), \quad (1)$$

where the parameters A_i and t_i were determined using the Levenberg–Marquardt least-squares algorithm of non-linear fit. The goodness of the fit was verified by the reduced χ^2 values, which ranged between 0.6 and 1.2 for all radiation qualities. The first and second HVLs were calculated with an iterative algorithm to solve x from Eq. (1) for $K_{\mathrm{air}} = K_0/2$ and $K_{\mathrm{air}} = K_0/4$, where K_0 is the air kerma measured without attenuation. The uncertainties were estimated as 3% and 4% for the first and second HVL, respectively.

2.2. Simulation

The X-ray production was simulated beginning with a beam of electrons impinging at an angle of 22° with the normal to the tungsten anode surface. A beryllium disc with the thickness of 2.2 mm, placed between the target and the region where the energy of the photon is registered, was used to simulate the inherent filtration. For each value of selected peak voltage (kVp), the spectrum of emitted photons from the target within an aperture angle of 30° was recorded in channels with width of 0.25 keV. The number of histories was chosen to produce statistical uncertainty of less than 5% for the total events contained in 1.0 keV interval centred at 90% of the maximum energy. Considering the spectrum with maximum energy of 100 keV, for example, the events of channels around 90 keV corresponding to 89.50, 89.75, 90.00 and 90.25 keV sum to 464 with statistical uncertainty of 4.6%. The calculations were run on a PC (Pentium IV, 2.4 GHz, 512 MB RAM, Linux) using 2×10^8 electrons that produced spectra with typical number of photons ranging from 5×10^4 (kVp = 20 kV) to 2×10^6 (kVp = 300 kV).

For each radiation quality, the filtration of the generated spectrum was simulated by directing the photon beam to one or more absorbers of Al, Cu, Sn and Pb with the thickness corresponding to that used in the experiment. The filtered spectrum was also recorded in channels with width of 0.25 keV. The low-energy extension of the electromagnetic processes provided by Geant4 was used in all simulations. More details about the simulation of X-ray production is described in Moralles et al. (2005).

2.3. Analysis

2.3.1. Half-value layers and attenuation curves

The first and second HVLs of the simulated spectra were calculated according to the procedure described by Ankerhold et al. (1999), using the absorption coefficients of Hubbell and Seltzer (1995). Simulated values have statistical uncertainties of less than 1%; errors of the cross-sections of the interactions used by Geant4 were not taken into account.

Table 1 presents results obtained from experiment, simulation and reference values. In general, the agreement of our experimental and simulated results with that of reference data is similar to those obtained by Seelentag et al. (1979) from measurements of X-ray spectra with a high-purity germanium detector.

According to criterion of ISO 4037-1 (ISO, 1997), *if the first and second HVLs in a given material agree within ±5% for two X-ray beams, then these two beams shall be considered to be essentially of the same quality*. Differences between experimental and simulated results for the first and second HVLs are shown in Fig. 1(a) and (b), respectively. Taking into account the uncertainties, one observes that five (N20, N25, N40, N60 and W200) of the 16 spectra have the first HVL with differences of more than 5%, and in the case of second HVL, only one spectrum (N60) does not agree within 5%. This result shows that the performance of Geant4 can be considered adequate to simulate the experiment.

Fig. 1(c) and (d) show the same comparisons between reference values and simulated results, considering statistical uncertainty of ±1%.

Table 1
First and second HVLs of X-ray with radiation qualities of the ISO narrow (N) and wide (W) spectrum series (ISO, 1997): results from experiment, simulation with Geant4, and reference values (ISO)

Quality	First HVL (mm)			Second HVL (mm)		
	Experiment	Simulation	ISO	Experiment	Simulation	ISO
N20	0.300	0.335	0.32	0.350	0.374	0.37
N25	0.584	0.635	0.66	0.680	0.708	0.73
N30	1.05	1.12	1.15	1.24	1.22	1.30
N40	0.073	0.082	0.084	0.089	0.089	0.091
N60	0.245	0.222	0.24	0.300	0.249	0.26
N80	0.560	0.550	0.58	0.617	0.594	0.62
N100	1.10	1.04	1.11	1.10	1.10	1.17
N120	1.62	1.64	1.71	1.71	1.70	1.77
N200	3.60	3.86	3.99	3.63	3.93	4.05
N250	4.99	5.10	5.19	5.15	5.14	5.23
N300	5.68	5.95	6.12	5.73	5.99	6.15
W80	0.358	0.332	0.35	0.425	0.411	0.44
W110	0.905	0.901	0.96	1.00	1.04	1.11
W150	1.81	1.73	1.86	2.00	1.95	2.10
W200	3.17	2.90	3.08	3.23	3.14	3.31
W250	4.41	4.07	4.22	4.62	4.26	4.40

Aluminium is used as attenuator material for N20, N25 and N30 radiation qualities. Copper is used for the others.

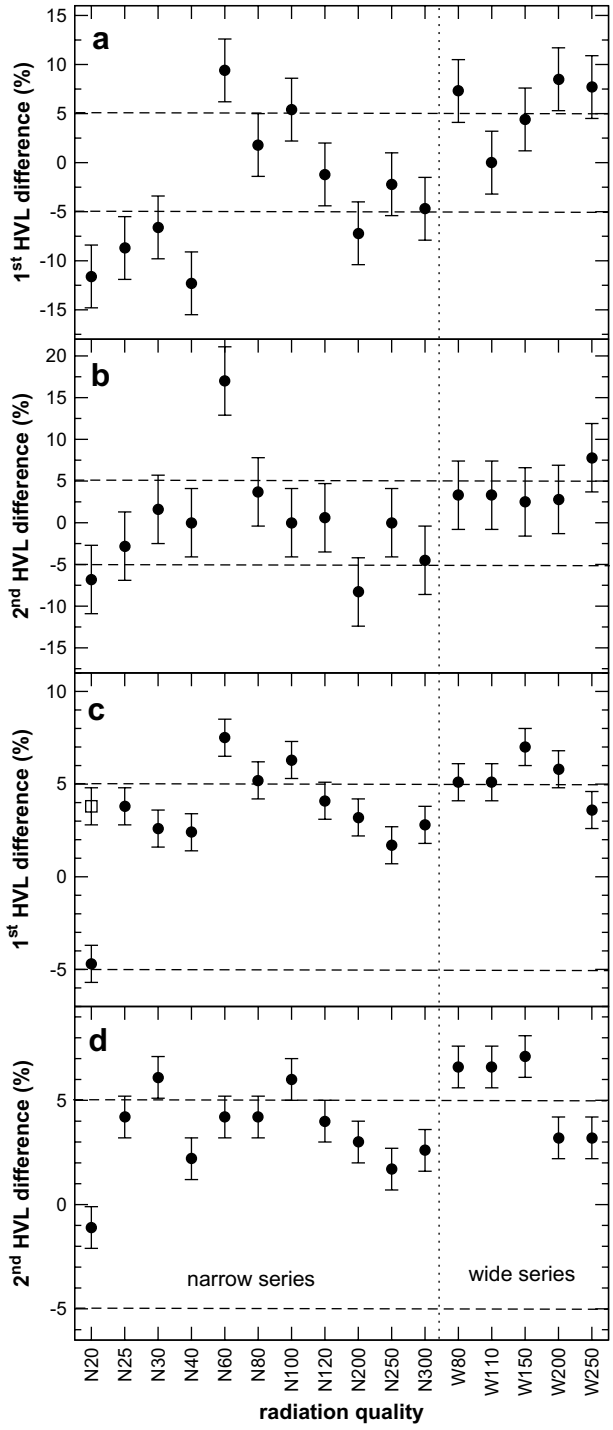

Fig. 1. Differences in HVLs between results of: (a) experiment and simulation, 1st HVL; (b) experiment and simulation, 2nd HVL; (c) reference (ISO, 1997) and simulation, 1st HVL; (d) reference and simulation, 2nd HVL. Horizontal segmented lines indicate the difference range between ±5%. The open square point in (c) corresponds to the difference between simulation and the result of Ankerhold et al. (1999) for N20 (see text).

In this case, results of six spectra (N30, N60, N100, W80, W110 and W150) do not comply with the ISO requirements. Furthermore, one observes that the discrepancies show a systematic behaviour, since almost all HVLs obtained in the simulations are smaller than the reference values. This is an indication that the simulated spectra have more contributions from low-energy photons when compared with the reference spectra. Considering that the ISO report does not specify the exact values for anode angle, inherent

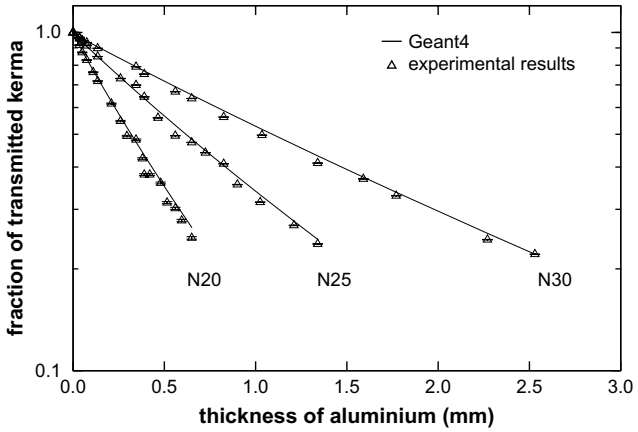

Fig. 2. Transmission curves obtained with simulated spectra and experimental points for ISO narrow series using aluminium absorbers.

filtration and thickness of air that they used, it is expected that X-ray spectra produced with different values of these parameters present systematic changes in comparison with the reference spectra. The particular combination of these parameters in the experimental setup, which are probably not the same of that employed to establish the reference values, could be the cause of the abundance of low-energy photons in the simulated spectra.

The result for radiation quality N20 deserves some comments, since Fig. 1(c) shows that the difference for N20 is quite far from the systematic behaviour presented by the other radiation qualities. The more recent ISO 4037-4 (ISO, 2004) presents corrected values for the mean energies of N15, N20 and N30 radiation qualities that were taken from the work of Ankerhold et al. (1999). These authors measured mean energy and first HVL for N20 that are 2.5 and 9% greater than the values presented in the ISO 4037-1, respectively. If the HVL value measured by Ankerhold (0.348 mm Al) is used instead of the ISO 4037-1 value (0.32 mm Al), the difference from the value obtained by simulation (0.335 mm Al) for N20 changes from −4.7 to +3.7%, which is compatible with the average difference of the other radiation qualities, as shown by the open square point in Fig. 1(c). Results for N30 do not show significative changes.

Besides the HVL values, attenuation curves provide useful information that are influenced by the shapes of the spectra. Figs. 2 and 3 show comparisons of transmitted kerma curves for aluminium and copper attenuators, respectively. One observes reasonable agreement between the attenuation obtained with the simulated spectra and experimentally. In fact, the data reveal an

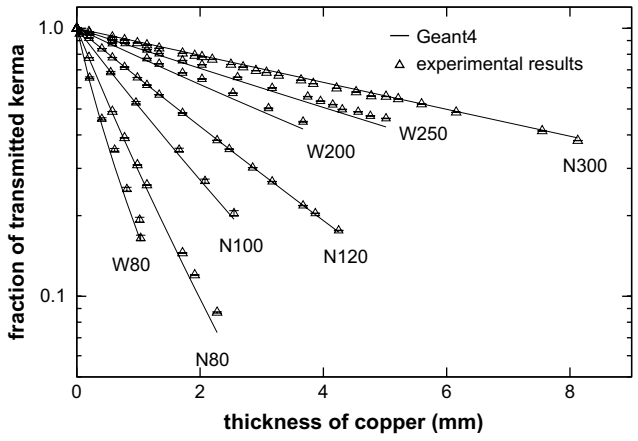

Fig. 3. Transmission curves obtained with simulated spectra and experimental points for ISO narrow and wide series using copper absorbers.

Table 2
Mean energy and spectral resolution of narrow (N) and wide (W) radiation qualities of simulated spectra and ISO reference (ISO, 1997; ISO, 2004)

Quality	Mean energy (keV)		Resolution (%)	
	Simulated	ISO	Simulated	ISO
N20	15.9	16.4[a]	33.4	34
N25	19.9	20.4[a]	33.7	33
N30	24.2	24.7[a]	33.9	32
N40	32.8	33	30.2	30
N60	47.0	48	37.9	36
N80	64.0	65	32.3	32
N100	82.9	83	28.2	28
N120	99.3	100	28.0	27
N200	163.0	164	29.9	30
N250	206.8	208	26.8	28
N300	249.4	250	27.2	27
W60	44.1	45	46.5	48
W80	55.5	57	51.5	55
W110	77.9	79	49.8	51
W150	102.6	104	55.0	56
W200	135.0	137	53.8	57
W250	170.3	173	54.9	56

Typical uncertainties of mean energies and spectral resolutions of the simulated spectra are 0.1 and 1%, respectively.
[a] Taken from reference (ISO, 2004).

average difference of 4% between experimental points and simulated data. We attribute the main contribution for these discrepancies to impurities that must be present in additional filters and in the copper absorbers. Previous studies concerning the influence of impurities in the attenuators used in HVL measurements reported similar average differences (Wagner et al., 1990; Terry et al., 1999).

2.3.2. Mean energy and resolution

Table 2 presents mean energy and spectral resolution of the simulated spectra as defined in the ISO specifications (ISO, 1997). Since the inherent filtration of the tube is 2.2 mm beryllium, this reference states that the agreement must be within ±5 and ±15% for mean energy and spectral resolution, respectively. The differences in these parameters between results from simulated spectra and reference values are presented in Fig. 4. One observes that all simulated spectra obey the ISO conditions. However, the mean energies of the simulated spectra are systematically lower than that of reference values. This is another indication that, in comparison with the ISO reference, the spectra obtained by simulation contain more contributions from low-energy photons.

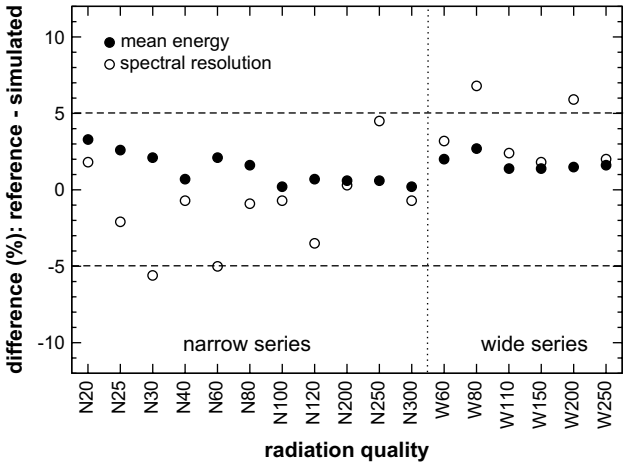

Fig. 4. Differences in mean energy and spectral resolution between reference values and simulated spectra and reference values. Uncertainties are of the order or smaller than the point size. Horizontal segmented lines indicate the difference range between ±5%.

The fact that all simulated spectra obey the ISO requirements concerning the mean energy and spectral resolution but many of them fail to obey the HVL conditions indicates that these requirements are not equivalent in practice.

3. Conversion coefficients

The conversion coefficient $h(d, \alpha)$ for photons incident on phantoms is defined by

$$h(d,\alpha) = \frac{H_p(d,\alpha)}{K_{air}} \quad (2)$$

where $H_p(d, \alpha)$ is the personal dose equivalent at depth d and angle α of radiation incidence on the dosimeter, and K_{air} the air kerma free-in-air. Recommended conversion coefficients for slab phantom are published in the ISO reference (ISO, 1999) for narrow and wide spectrum series. In this section we report the conversion coefficients calculated with the Geant4 for the ICRU tissue-equivalent and ISO water slab phantoms at the depth of 10 mm, and compare them with ISO reference values.

3.1. Simulation

The kerma-to-dose equivalent conversion coefficients were calculated for two types of phantoms: ICRU slab phantom (ICRU, 1998) and ISO water slab phantom (ISO, 1999). In the simulation,

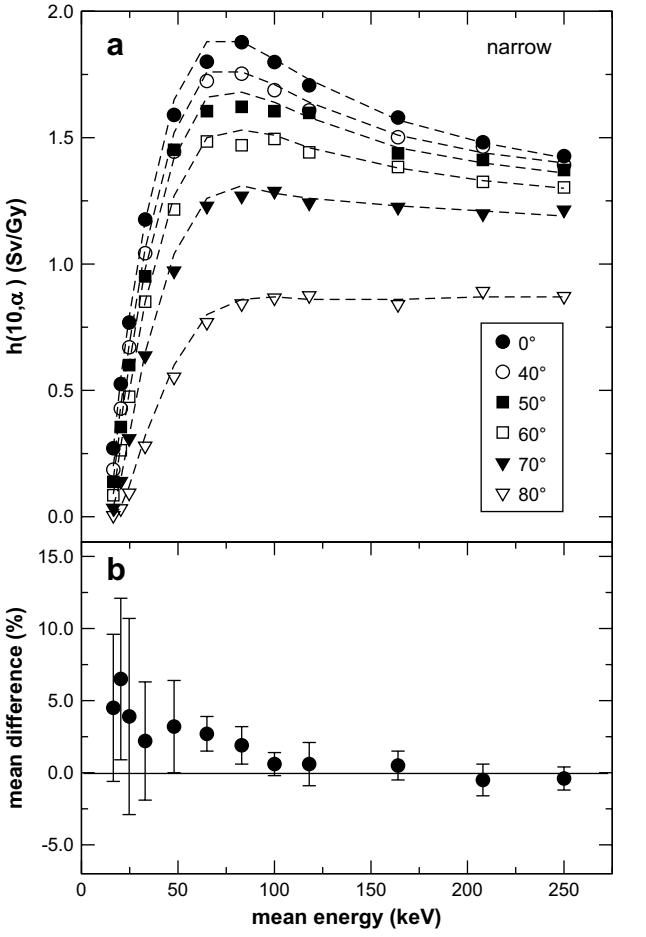

Fig. 5. (a) Conversion coefficients $h(10, \alpha)$ of the ISO narrow spectra simulated with Geant4 toolkit for the ICRU tissue-equivalent solid slab at several incidence angles α. Segmented lines represent $h(10, \alpha)$ reference values (ISO, 1999). (b) Mean differences (Eq. (5)) over all angles. Dispersions (Eq. (6)) are indicated by error bars.

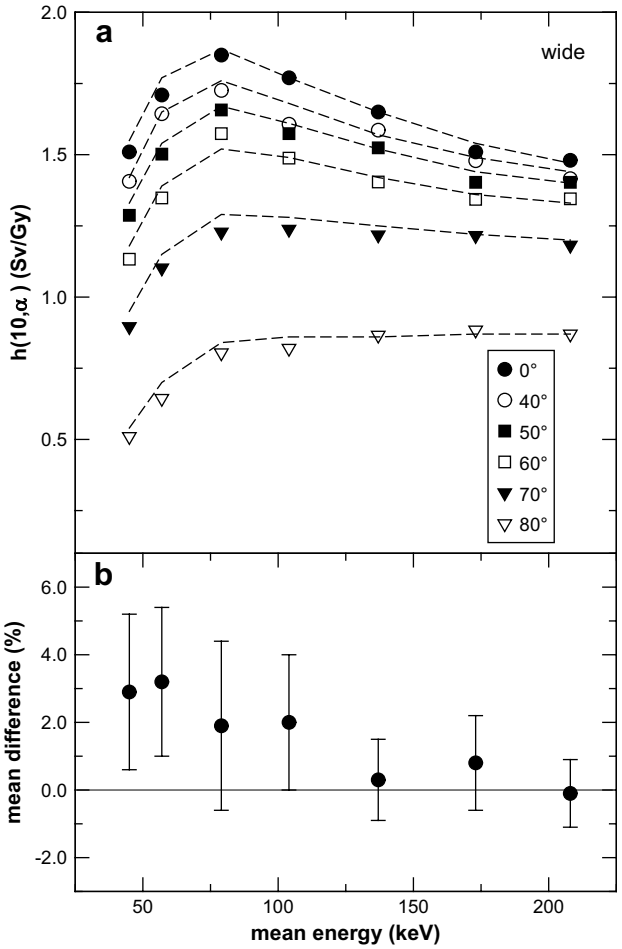

Fig. 6. (a) Conversion coefficients $h(10, \alpha)$ of the ISO narrow spectra simulated with Geant4 toolkit for the ICRU tissue-equivalent solid slab at several incidence angles α. Segmented lines represent $h(10, \alpha)$ reference values (ISO, 1999). (b) Mean differences (Eq. (5)) over all angles. Dispersions (Eq. (6)) are indicated by error bars.

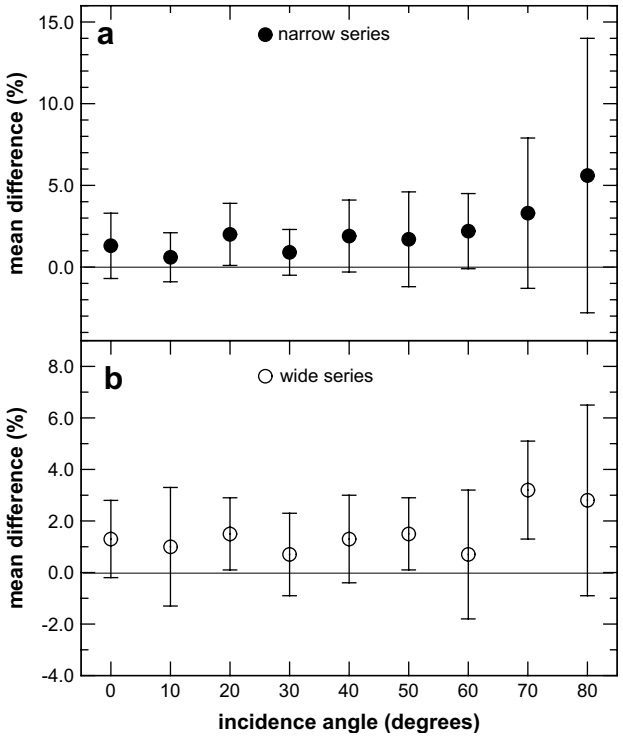

Fig. 7. Mean differences and dispersion (presented as error bars) between conversion coefficients obtained by simulation and reference (ISO, 1999) values for different angles. Results for the ICRU tissue-equivalent solid slab.

the ISO water slab phantom is a parallelepiped with walls of 10 mm thick except the frontal face of 2.5 mm thick made of polymethyl methacrylate (PMMA) with internal volume of $300 \times 300 \times 150\ \text{mm}^3$ full of water, whereas the ICRU slab phantom is a solid parallelepiped made of ICRU tissue-equivalent material having the same geometric dimension of the ISO water slab phantom. The energy distribution of the photons was taken from the spectra obtained in the simulation described in the previous section. The irradiation with several angles of incidence was simulated by rotating the phantom around the vertical axis that contains the centre of its frontal face.

The $H_p(10, \alpha)$ was evaluated by defining a square grid of 100×100 small spheres with radius of 0.25 mm, uniformly distributed on $63 \times 63\ \text{mm}^2$, and located at 10 mm from the outer surface of the frontal wall. The centre of the square grid of spheres coincides with the centre of the square radiation field. The total energy deposited in the 10,000 spheres divided by their total mass was used to represent the $H_p(10, \alpha)$ value. The energy deposition was obtained by using the method *GetTotalEnergyDeposit()* of Geant4. The K_{air} term of Eq. (2) corresponds to the air kerma free-in-air of the radiation field at the position of the phantom. It was evaluated by

$$K_{air} = \int_0^{E_{max}} \phi(E) \left(\frac{\mu(E)}{\rho}\right)_{air} dE, \tag{3}$$

where E_{max} is the maximum energy of the spectrum, $\phi(E)$ is the number of photons of energy E per unit of area, and $(\mu(E)/\rho)_{air}$ is the mass-energy absorption coefficient for photons of energy E in air, which was taken from Hubbell and Seltzer (1995). The number of primary photons used in the simulations was dependent on the radiation quality. It was chosen to produce values of $H_p(10, \alpha)$ with statistical uncertainties of less than 5%.

3.2. Analysis

3.2.1. ICRU tissue-equivalent slab phantom

The conversion coefficients for the ICRU tissue-equivalent slab phantom obtained by simulation are shown in Figs. 5(a) and 6(a) for narrow and wide spectra, respectively. Different symbols are used to distinguish each angle of photon incidence. For reasons of clarity, results for angles of 10°, 20° and 30° are not shown in the Figs. 5(a) and 6(a).

To analyse the agreement with reference values, the relative difference in percentage, $D_{r,\alpha}$, between reference $h'_{r,\alpha}$ and simulated $h_{r,\alpha}$ coefficients was calculated for each combination of parameters (r, α), according to

$$D_{r,\alpha} = 100 \frac{(h'_{r,\alpha} - h_{r,\alpha})}{h'_{r,\alpha}}, \tag{4}$$

where the parameters r and α refer to the radiation quality and irradiation angle, respectively. The general agreement for a specific spectrum series is obtained from the mean of all qualities and incidence angles of that series.

The agreement of the simulated results was then analysed relatively to the radiation quality and to the incidence angle by fixing one of the parameters and summing over the other to obtain the mean difference $\langle D_p \rangle$ for the fixed parameter p. For example, the calculation of the mean relative difference for the narrow spectrum with 60 kV ($r = \text{N60}$) is performed by

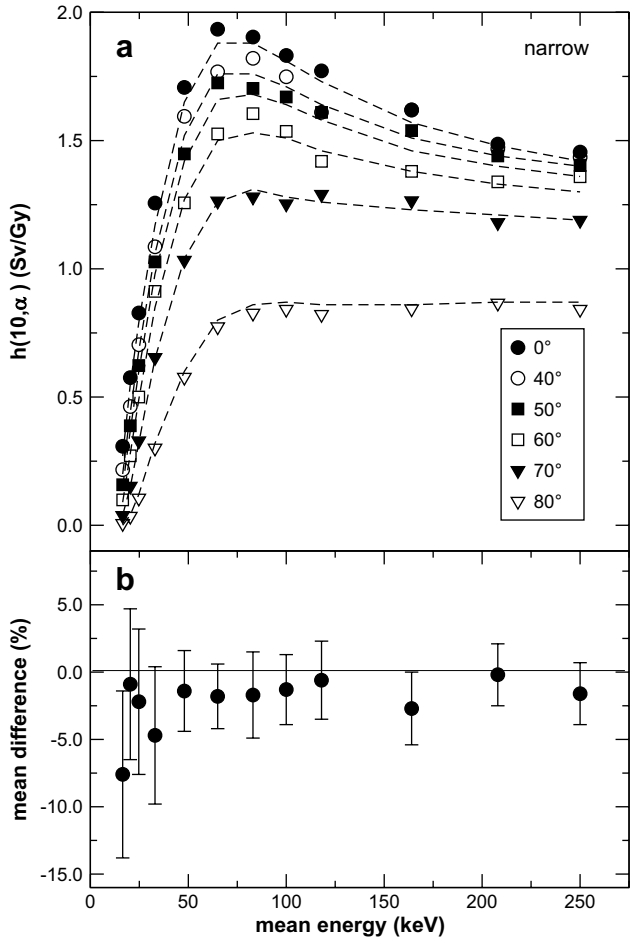

Fig. 8. (a) Conversion coefficients $h(10, \alpha)$ of the ISO narrow spectra simulated with Geant4 toolkit for the water slab phantom at several incidence angles α. Segmented lines represent $h(10, \alpha)$ reference values (ISO, 1999). (b) Mean differences (Eq. (5)) over all angles. Dispersions (Eq. (6)) are indicated by error bars.

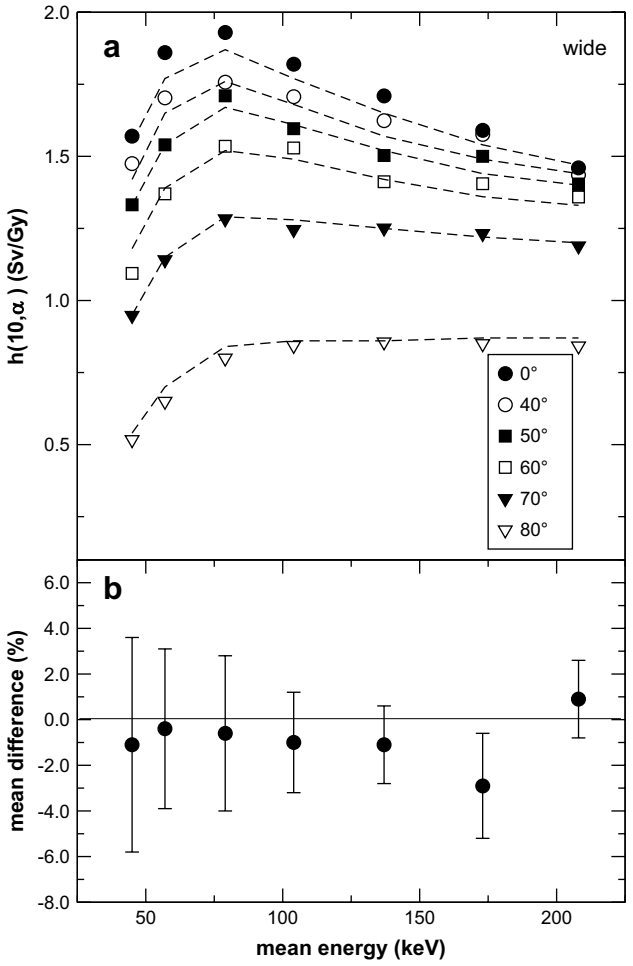

Fig. 9. (a) Conversion coefficients $h(10, \alpha)$ of the ISO wide spectra simulated with Geant4 toolkit for the water slab phantom at several incidence angles α. Segmented lines represent $h(10, \alpha)$ reference values (ISO, 1999). (b) Mean differences (Eq. (5)) over all angles. Dispersions (Eq. (6)) are indicated by error bars.

$$\langle D_{\mathrm{N60}} \rangle = \frac{100}{\mathrm{N}_\alpha} \times \sum_\alpha \frac{(h'_{\mathrm{N60},\alpha} - h_{\mathrm{N60},\alpha})}{h'_{\mathrm{N60},\alpha}}, \tag{5}$$

where α assumes $\mathrm{N}_\alpha = 9$ values, corresponding to the range from 0° to 80° in steps of 10°. Then, the standard deviation $\sigma_{D_{\mathrm{N60}}}$ of this difference, is calculated by

$$\sigma_{D_{\mathrm{N60}}} = \sqrt{\frac{\sum_\alpha (D_{\mathrm{N60},\alpha} - \langle D_{\mathrm{N60}} \rangle)^2}{\mathrm{N}_\alpha - 1}}. \tag{6}$$

The absolute value of the mean difference quantifies the amount that the simulated results disagree with the reference values, while the sign indicates overestimation (negative) or underestimation (positive). The standard deviation quantifies the dispersion of the mean differences.

The general percentages of the mean difference (dispersion) for narrow and wide spectra were 2.2% (3.8) and 1.6% (2.1), respectively. Figs. 5(b) and 6(b) present the mean differences with corresponding dispersions for fixed radiation qualities, while Fig. 7 shows the mean differences for fixed incidence angles. From these figures one observes that most of the mean differences are found within 1 and 3%. The exceptions with the largest discrepancies occur for spectra with lower mean energies (N20, N25, N30) and for large angles (70°, 80°). The predominance of positive differences indicates that the simulations produce conversion coefficients that are, in average, underestimated in relation to the ISO reference values. The origin of this underestimation is the abundance of low-energy photons as discussed in Section 2.3.2. The effect is more pronounced for the lower energy spectra due to the large attenuation of the primary photons, which reduces the number of photons that reach the depth of 10 mm. The differences diminish with increasing energy, as can be seen in Figs. 5(b) and 6(b). The same reasoning applies to the angular dependence shown in Fig. 7.

3.2.2. ISO water slab phantom

Figs. 8(a) and 9(a) show the conversion coefficients obtained by simulations (symbols) for the ISO water phantom as a function of the mean energy of the narrow and wide spectra, respectively, compared with reference values (segmented lines) (ISO, 1999). For clarity, results for angles of 10°, 20° and 30° are not shown.

The general percentage of the mean difference (dispersion) in comparison with the ISO reference was −2.2% (4.2) and −0.9% (3.0) for narrow and wide spectra, respectively. The absolute values of these differences are similar to those obtained for the ICRU tissue-equivalent phantom, but the signs are opposite. Figs. 8(b) and 9(b) show the mean differences and dispersions of narrow and wide spectra, respectively. In this case almost all differences are negative, indicating that the coefficients calculated with Geant4 for this phantom are overestimated in relation to the reference. Negative mean differences are observed also for fixed angles from 0° to 60°, shown in Fig. 10. The reason for this overestimation is that in the

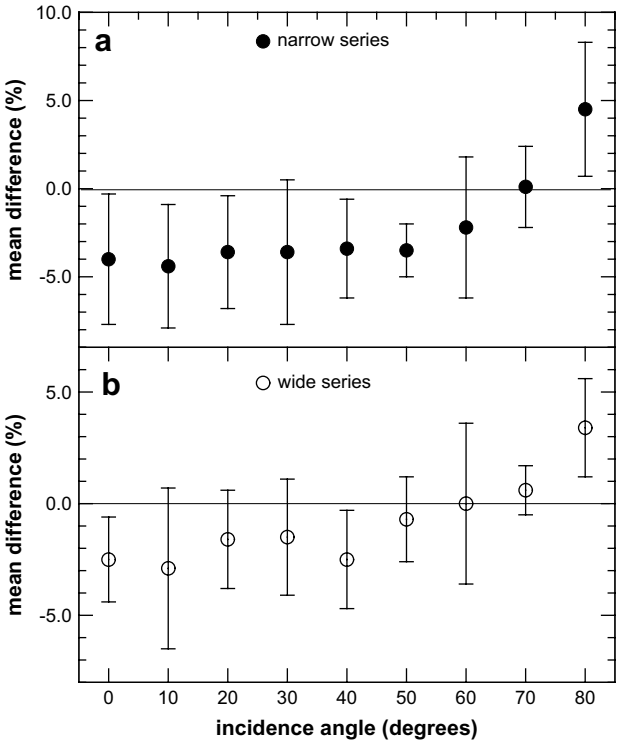

Fig. 10. Mean differences and dispersion (presented as error bars) between conversion coefficients obtained by simulation and reference (ISO, 1999) values for different angles. Results for the water slab phantom.

water slab phantom more photons reach the depth of 10 mm than in the ICRU slab phantom. Differences between the backscatter factors for these two phantoms, which were extensively studied by Traub et al. (1997), explain that the conversion coefficients for the ISO water slab phantom are larger than for the ICRU tissue slab phantom.

4. Conclusion

The results of this work show that narrow and wide X-ray spectra produced with Geant4 present mean energy and resolution that agree with that of reference radiations. Furthermore, the HVLs of the simulated spectra are compatible with experimental results within the uncertainties. The simulation of spectra with lower values of mean energies and HVLs reveals that Geant4 presents a small tendency to produce more photons of low energy than the corresponding reference spectra.

The results of our simulations show that almost all conversion coefficients of the ISO reference (ISO, 1999) lie between the results obtained with the ICRU tissue-equivalent slab phantom and the ISO water slab phantom.

The conversion coefficients calculated with Geant4 present differences of the order of 1–3% when compared with reference values for most of the radiation qualities and incidence angles. The observation of larger differences for low energies and large incidence angles can be a motivation for calculations with other Monte Carlo codes in order to determine if the origin of these discrepancies lie in the mathematical treatment of the physical processes or in the cross-section data.

In summary, Geant4 seems adequate to be employed in simulations of dosimetry of photons with energies of ten to a few hundreds of keV.

Acknowledgement

C.C. Guimarães thanks CAPES (Brazil) for a scholarship.

References

Agostinelli, S., Allison, J., Amako, K., et al., 2003. GEANT4 – a simulation toolkit. Nucl. Instrum. Methods A 506, 250–303.

Ankerhold, U., Behrens, B., Ambrosi, P., 1999. X ray spectrometry of low energy photons for determining conversion coefficients from air kerma, K_a, to personal dose equivalent, $H_p(10)$, for radiation qualities of the ISO narrow spectrum series. Radiat. Prot. Dosimetry 81, 247–258.

Ankerhold, U., 2007. X reference radiation qualities produced with tube voltages above 300 kV for the calibration and testing of dosemeters. Radiat. Prot. Dosimetry 123, 137–142.

Grosswendt, B., 1991a. The influence of the photon beam direction on the dose equivalent in the IAEA 30 cm water cube phantom. Radiat. Prot. Dosimetry 35, 5–12.

Grosswendt, B., 1991b. The angular dependence and irradiation geometry factor for the dose equivalent for photons in slab phantoms of tissue-equivalent material and PMMA. Radiat. Prot. Dosimetry 35, 221–235.

Grosswendt, B., 1992. Coefficients for the conversion of air collision kerma to dose equivalent for the calibration of individual dosemeters in X ray fields. Radiat. Prot. Dosimetry 40, 169–184.

Hubbell, J.H., Seltzer, S.M., 1995. Tables of mass attenuation coefficients and mass energy absorption coefficients 1 keV to 20 MeV for elements $Z=1$ to 92 and 48 additional substances of dosimetric interests. NIST, NISTIR 5632. Updated versions of these tables are presently available from: http://physics.nist.gov/.

ICRU, 1998. Conversion Coefficients for Use in Radiological Protection Against External Radiation. ICRU Report 57. ICRU Publications, Bethesda, MD.

ISO, 1997. X and Gamma Reference Radiations for Calibrating Dosemeters and Doserate Meters and for Determining Their Response as a Function of Photon Energy – Part 1: Radiation Characteristics and Production Methods. ISO 4037-1, Geneva, Switzerland.

ISO, 1999. X and Gamma Reference Radiations for Calibrating Dosemeters and Doserate Meters and for Determining Their Response as a Function of Photon Energy – Part 3: Calibration of Area and Personal Dosemeters and the Measurement of their Response as a Function of Energy and Angle of Incidence. ISO 4037-3, Geneva, Switzerland.

ISO, 2004. X and Gamma Reference Radiations for Calibrating Dosemeters and Doserate Meters and for Determining Their Response as a Function of Photon Energy – Part 4: Calibration of Area and Personal Dosemeters in Low Energy X Reference Radiation Fields. ISO 4037-4, Geneva, Switzerland.

Mikami, S., Itié, C., Texier, C., 2007. Consideration on calibration and correction factors of an $H_p(10)$ chamber for different radiation qualities and angles of incidence. Radiat. Prot. Dosimetry 123, 122–127.

Moralles, M., Guimarães, C.C., Okuno, E., 2005. Response of thermoluminescent dosemeters to photons simulated with the Monte Carlo method. Nucl. Instrum. Methods A 545, 261–268.

Seelentag, W.W., Panzer, W., Drexler, G., Platz, L., Santner, F.A. Catalogue of Spectra for the Calibration of Dosemeters. GSF-Bericht 560.

Terry, J.A., Waggener, R.G., Miller Blough, M.A., 1999. Half-value layer and intensity variations as a function of position in the radiation field for film-screen mammography. Med. Phys. 26, 259–266.

Traub, R.J., McDonald, J.C., Murphy, M.K., 1997. Determination of photon backscatter from several calibration phantoms. Radiat. Prot. Dosimetry 74, 13–20.

Wagner, L.K., Archer, B.R., Cerra, F., 1990. On the measurement of half-value layer in film-screen mammography. Med. Phys. 17, 989–997.